Scalar meson spectroscopy with a fine lattice

FU Zi-Wen(傅子文)[1;1)] Carleton DeTar[2;2)]

[1] Key Laboratory of Radiation Physics and Technology (Sichuan University), Ministry of Education; Institute of Nuclear Science and Technology, Sichuan University, Chengdu 610064, China
[2] Physics Department, University of Utah, Salt Lake City, UT 84112, USA

Abstract: With sufficiently light u and d quarks the isovector (a_0) and isosinglet (f_0) scalar meson propagators are dominated at large distances by two-meson states. In the staggered fermion formulation of lattice QCD, taste-symmetry breaking causes a proliferation of multihadron states that complicates the analysis of these channels. Of special interest is the bubble contribution, which makes a considerable contribution to these channels. Using numerical simulation we have measured the correlators for both a_0 and f_0 channels in the "Asqtad" improved staggered fermion formulation in a MILC fine ($a = 0.09$ fm) lattice ensemble. We analyze those correlators using rooted staggered chiral perturbation theory (rSχPT) and achieve chiral couplings that are well consistent with previous determinations.

Key words: lattice QCD, scalar meson, bubble contribution

PACS: 11.15.Ha, 12.38.Gc, 12.39.Fe **DOI:** 10.1088/1674-1137/35/10/002

1 Introduction

The recent evident successes of lattice QCD simulations with improved staggered fermions demand an intensive examination of the "fourth-root trick" using fractional powers of the determinant to simulate the correct number of quark species. This trick automatically performs the transition from four tastes to one taste per flavor for staggered fermions at all orders. The procedure is known to introduce nonlocalities and violations of unitarity at nonzero lattice spacing [1]. Hence there are strong theoretical arguments [2–5] that the fourth-root trick is valid.

One can test the fourth-root trick numerically [6–12]. Alternatively, low-energy results of staggered fermion QCD simulations can be compared with predictions of rSχPT [13, 14]. Since staggered chiral perturbation theory becomes standard chiral perturbation theory in the continuum limit, agreement between rooted QCD and rSχPT at nonzero lattice spacing would suggest that lattice artifacts produced by the fourth-root approximation are innocuous. There are two recent tests of agreement between rooted staggered fermion QCD and rSχPT [15, 16].

The a_0 channel has been studied in staggered fermion QCD. An explanation of the nonstandard features of the scalar correlators is provided by rSχPT [17–19]. In that theory all pseudoscalar mesons come in multiplets of 16 tastes. The π and K multiplets are split in similar ways. For η and η' mesons only the taste singlet η and η' obtain physical mass. Some of the remaining members of the η multiplet remain degenerate with the pions. According to taste symmetry selection rules, any two mesons coupling to a taste-singlet a_0 must have the same taste. All tastes are equally allowed. Among other states, the taste singlet a_0 couples to the Goldstone pion (pseudoscalar taste) and an η, also with pseudoscalar taste and of the same mass. This two-body state at twice the mass of the Goldstone boson accounts for the anomalous low-energy component in that channel.

In our previous work we extended the analysis of Refs. [18, 19], examined the scalar meson correlators in full QCD on a MILC coarse ($a = 0.12$ fm) lattice ensemble and compared their two-meson content with predictions of rSχPT [20, 21]. Since the appearance of the two-meson intermediate state (i.e. bubble contribution) is a consequence of the fermion determinant, an analysis of this correlator gives a direct test of the fourth root recipe. In this work we extend

Received 8 December 2010, Revised 6 January 2011

1) E-mail: fuziwen@scu.edu.cn
2) E-mail: detar@physics.utah.edu

the analysis of Refs. [20, 21] and carry out a quantitative comparison of the measured correlators and the predictions of rSχPT at a fine ($a = 0.09$ fm) lattice ensemble. Despite the considerable complexity of channels with dozens of spectral components, the chiral theory models the correlators precisely in terms of only a small number of chiral couplings, which we may determine through fits to the data [20, 21].

2 Pseudoscalar meson taste multiplets

In Refs. [20, 21] we give a brief review of the rooted staggered chiral perturbation theory with particular focus on the tree-level pseudoscalar mass spectrum, and achieve the rooted version of the theory through the replicated theory [22].

The tree-level masses of the pseudoscalar mesons are [13, 21]

$$M^2_{\mathrm{ff}'_b} = B_0(m_{\mathrm{f}} + m_{\mathrm{f}'}) + a^2\Delta_b, \tag{1}$$

where ff′ are two flavors which make up, $b = 1, \cdots, 16$ are the taste, $B_0 = m_\pi^2/2m_{\mathrm{q}}$ is the coupling constant of the point scalar current to the pseudoscalar field, and the term of $a^2\Delta_b$ comes from taste-symmetry breaking.

In this work we investigate degenerate u and d quarks ($m_{\mathrm{u}} = m_{\mathrm{d}}$), so it will be convenient to introduce the notation

$$\begin{aligned} M^2_{\mathrm{Ub}} &= 2B_0 m_{\mathrm{u}} + a^2\Delta_b, \\ M^2_{\mathrm{Sb}} &= 2B_0 m_{\mathrm{s}} + a^2\Delta_b, \\ M^2_{\mathrm{Kb}} &= B_0(m_{\mathrm{u}} + m_{\mathrm{s}}) + a^2\Delta_b. \end{aligned} \tag{2}$$

The isosinglet states (η and η′) are modified both by the taste-singlet anomaly and by the two-trace (quark-line hairpin) taste-vector and taste-axial-vector operators [17, 23]. When the anomaly parameter m_0 is large, we obtain the usual result

$$M^2_{\eta,\mathrm{I}} = \frac{1}{3}M^2_{\mathrm{UI}} + \frac{2}{3}M^2_{\mathrm{SI}}, \quad M_{\eta',\mathrm{I}} = \mathcal{O}(m_0^2). \tag{3}$$

In the taste-axial-vector sector we have

$$\begin{aligned} M^2_{\eta\mathrm{A}} &= \frac{1}{2}\left[M^2_{\mathrm{UA}} + M^2_{\mathrm{SA}} + \frac{3}{4}\delta_{\mathrm{A}} - Z_{\mathrm{A}}\right], \\ M^2_{\eta'\mathrm{A}} &= \frac{1}{2}\left[M^2_{\mathrm{UA}} + M^2_{\mathrm{SA}} + \frac{3}{4}\delta_{\mathrm{A}} + Z_{\mathrm{A}}\right], \\ Z^2_{\mathrm{A}} &= (M^2_{\mathrm{SA}} - M^2_{\mathrm{UA}})^2 - \frac{\delta_{\mathrm{A}}}{2}(M^2_{\mathrm{SA}} - M^2_{\mathrm{UA}}) + \frac{9}{16}\delta^2_{\mathrm{A}}, \end{aligned} \tag{4}$$

where δ_V is the hairpin coupling of a pair of taste-vector mesons, δ_{A} is the hairpin coupling of a pair of taste-axial mesons [17].

In the taste-pseudoscalar and taste-tensor sectors, in which there is no mixing of the isosinglet states, the masses of the η_{b} and η'_{b} by definition are

$$M^2_{\eta,\mathrm{b}} = M^2_{\mathrm{Ub}}; \quad M^2_{\eta',\mathrm{b}} = M^2_{\mathrm{Sb}}. \tag{5}$$

In Table 1 we list the masses of the resulting taste multiplets in lattice units for the lattice ensemble used in the present study with taste-breaking parameters δ_{A} and δ_{V} determined in Refs. [15, 17] as measured or inferred from the measured masses and splittings. The mass of the η'_{I} depends on m_0.

Table 1. Mass spectrum of pseudoscalar meson for the MILC fine ($a = 0.09$ fm) lattice ensemble $\beta = 7.09$, $am_{\mathrm{ud}} = 0.0062$, $am_{\mathrm{s}} = 0.031$.

b	$a\pi_b$	aK_b	$a\eta_b$	$a\eta'_b$
P	0.1479	0.2532	0.1479	0.3273
A	0.1646	0.2633	0.1530	0.3325
T	0.1743	0.2695	0.1743	0.3400
V	0.1820	0.2745	0.1780	0.3430
I	0.1926	0.2816	0.3064	—

3 Scalar correlators from SχPT

In Refs. [20, 21], using the language of the replica trick [13, 24] and through matching the point-to-point scalar correlators in chiral low energy effective theory and staggered fermion QCD, we rederive the "bubble" contribution to the a_0 channel of Ref. [19], and then extend the result to the f_0 channel. Here we just review some results required for this work.

3.1 Isovector a_0 correlator

For simplicity we consider the $\mathrm{u\bar{d}}$ flavor state for the a_0 correlator. Only the quark-line-connected contribution appears in the QCD correlator. The time-slice correlator for the a_0 meson is given by,

$$C(\boldsymbol{p}, t) = \sum_{\boldsymbol{x}} \mathrm{e}^{\mathrm{i}\boldsymbol{p}\cdot\boldsymbol{x}} \langle \bar{d}(\boldsymbol{x}, t) u(\boldsymbol{x}, t) \bar{u}(0,0) d(0,0) \rangle, \tag{6}$$

where $\boldsymbol{p}$ is the chosen momentum. There exist many multihadron states with $J^P = 0^+$ and $I = 1$ which can propagate between the source and the sink. Of special interest in multihadron states is the intermediate state with two pseudoscalars P_1 P_2 which we refer to as the bubble contribution (B) [19]. If the masses of P_1 and P_2 are small, the bubble contribution B gives a considerable contribution to the a_0 correlator, and it should be included in the fit of the lattice correlator in Eq. (6), that is,

$$C(\boldsymbol{p}, t) = A\mathrm{e}^{-m_{\mathrm{a}_0} t} + B_{\mathrm{a}_0}(\boldsymbol{p}, t), \tag{7}$$

where for notational simplicity we omit the contributions from the excited a_0 meson; the oscillating terms correspond to a particle with opposite parity, and other high-order multihadron intermediate states.

The $B_{a_0}(\boldsymbol{p},t)$ is in detail denoted in Appendix B of Ref. [20]. For 1+1+1 theory, if we rearrange the terms of the time Fourier transform of bubble correlator in Eq. (53) in Ref. [21], we obtain

$$B_{a_0}(\boldsymbol{p},t)=\frac{B_0^2}{4L^3}\left\{f_{\rm B}(\boldsymbol{p},t)+f_{\rm V}^{\rm hairpin}(\boldsymbol{p},t)+f_{\rm A}^{\rm hairpin}(\boldsymbol{p},t)\right\},$$

where $B_0=\dfrac{m_\pi^2}{2m_{\rm u}}$ is the coupling constant of the point scalar current to the pseudoscalar field, and

$$\begin{aligned}
&f_{\rm V}^{\rm hairpin}(\boldsymbol{p},t)\\
&\equiv\sum_{\boldsymbol{k}}\left\{-8\frac{{\rm e}^{-\left(\sqrt{(\boldsymbol{p}+\boldsymbol{k})^2+M_{\rm U_V}^2}+\sqrt{\boldsymbol{k}^2+M_{\rm U_V}^2}\right)t}}{\sqrt{(\boldsymbol{p}+\boldsymbol{k})^2+M_{\rm U_V}^2}\sqrt{\boldsymbol{k}^2+M_{\rm U_V}^2}}\right.\\
&\quad+4C_{\rm V_\eta}\frac{{\rm e}^{-\left(\sqrt{(\boldsymbol{p}+\boldsymbol{k})^2+M_{\rm \eta V}^2}+\sqrt{\boldsymbol{k}^2+M_{\rm \eta V}^2}\right)t}}{\sqrt{(\boldsymbol{p}+\boldsymbol{k})^2+M_{\rm \eta V}^2}\sqrt{\boldsymbol{k}^2+M_{\rm \eta V}^2}}\\
&\quad\left.-4C_{\rm V_{\eta'}}\frac{{\rm e}^{-\left(\sqrt{(\boldsymbol{p}+\boldsymbol{k})^2+M_{\rm \eta' V}^2}+\sqrt{\boldsymbol{k}^2+M_{\rm \eta' V}^2}\right)t}}{\sqrt{(\boldsymbol{p}+\boldsymbol{k})^2+M_{\rm \eta' V}^2}\sqrt{\boldsymbol{k}^2+M_{\rm \eta' V}^2}}\right\},
\end{aligned}$$

$$\begin{aligned}
f_{\rm B}(\boldsymbol{p},t)\equiv&\sum_{\boldsymbol{k}}\left\{\frac{2}{3}\frac{{\rm e}^{-\left(\sqrt{(\boldsymbol{p}+\boldsymbol{k})^2+M_{\rm \eta I}^2}+\sqrt{\boldsymbol{k}^2+M_{\rm \eta I}^2}\right)t}}{\sqrt{(\boldsymbol{p}+\boldsymbol{k})^2+M_{\rm \eta I}^2}\sqrt{\boldsymbol{k}^2+M_{\rm \eta I}^2}}\right.\\
&-2\frac{{\rm e}^{-\left(\sqrt{(\boldsymbol{p}+\boldsymbol{k})^2+M_{\rm U_I}^2}+\sqrt{\boldsymbol{k}^2+M_{\rm U_I}^2}\right)t}}{\sqrt{(\boldsymbol{p}+\boldsymbol{k})^2+M_{\rm U_I}^2}\sqrt{\boldsymbol{k}^2+M_{\rm U_I}^2}}\\
&+\frac{1}{8}\sum_{b=1}^{16}\frac{{\rm e}^{-\left(\sqrt{(\boldsymbol{p}+\boldsymbol{k})^2+M_{\rm U_b}^2}+\sqrt{\boldsymbol{k}^2+M_{\rm U_b}^2}\right)t}}{\sqrt{(\boldsymbol{p}+\boldsymbol{k})^2+M_{\rm U_b}^2}\sqrt{\boldsymbol{k}^2+M_{\rm U_b}^2}}\\
&\left.+\frac{1}{16}\sum_{b=1}^{16}\frac{{\rm e}^{-\left(\sqrt{(\boldsymbol{p}+\boldsymbol{k})^2+M_{\rm K_b}^2}+\sqrt{\boldsymbol{k}^2+M_{\rm K_b}^2}\right)t}}{\sqrt{(\boldsymbol{p}+\boldsymbol{k})^2+M_{\rm K_b}^2}\sqrt{\boldsymbol{k}^2+M_{\rm K_b}^2}}\right\},
\end{aligned}\tag{8}$$

where

$$C_{\rm V_\eta}=\frac{(M_{\rm S_V}^2-M_{\rm U_V}^2-\frac{1}{4}\delta_{\rm V}+Z_{\rm V})}{Z_{\rm V}},\tag{9}$$

$$C_{\rm V_{\eta'}}=\frac{(M_{\rm S_V}^2-M_{\rm U_V}^2-\frac{1}{4}\delta_{\rm V}-Z_{\rm V})}{Z_{\rm V}},\tag{10}$$

$M_{\rm \eta V}$, $M_{\rm \eta A}$, $M_{\rm \eta' V}$, $M_{\rm \eta' A}$, $Z_{\rm V}$, $Z_{\rm A}$ are given in Eq. 5, and for $f_{\rm A}^{\rm hairpin}(t)$, we just require $\rm V\to A$ in $f_{\rm V}^{\rm hairpin}(t)$.

3.2 Isosinglet f_0 correlator

We use the isosinglet operator for the f_0 correlator. Both quark-line-connected and quark-line-disconnected contributions appear in the lattice QCD correlator. The timeslice correlator for the f_0 meson is given by,

$$\begin{aligned}
C(\boldsymbol{p},t)=&\sum_{\boldsymbol{x}}{\rm e}^{{\rm i}\boldsymbol{p}\cdot\boldsymbol{x}}\langle\bar u(\boldsymbol{x},t)u(\boldsymbol{x},t)\bar u(0,0)u(0,0)\rangle_{\rm CC}\\
&+\frac{1}{2}\sum_{\boldsymbol{x}}{\rm e}^{{\rm i}\boldsymbol{p}\cdot\boldsymbol{x}}\langle\bar u(\boldsymbol{x},t)u(\boldsymbol{x},t)\bar u(0,0)u(0,0)\rangle_{\rm DC},
\end{aligned}\tag{11}$$

where the subscript CC stands for the connected contribution, and the subscript DC stands for the disconnected contribution. Like the a_0 correlator the bubble term of the scalar f_0 correlator also gives a considerable contribution, and it should be included in the fit of the lattice correlator in Eq. (11),

$$C(\boldsymbol{p},t)=A{\rm e}^{-m_{\rm f_0}t}+B_{\rm f_0}(\boldsymbol{p},t).\tag{12}$$

The $B_{\rm f_0}(t)$ is in detail denoted in Appendix C in Ref. [20]. For 1+1+1 theory, if we rearrange the terms of the time Fourier Transform of bubble correlator in Eq. (64) in Ref. [21], we obtain

$$B_{\rm f_0}(\boldsymbol{p},t)=\frac{B_0^2}{4L^3}\left\{f_{\rm B}(\boldsymbol{p},t)+f_{\rm V}^{\rm hairpin}(\boldsymbol{p},t)+f_{\rm A}^{\rm hairpin}(\boldsymbol{p},t)\right\}$$

and

$$\begin{aligned}
&f_{\rm V}^{\rm hairpin}(\boldsymbol{p},t)\\
&\equiv\sum_{\boldsymbol{k}}\left\{-4\frac{{\rm e}^{-\left(\sqrt{(\boldsymbol{p}+\boldsymbol{k})^2+M_{\rm U_V}^2}+\sqrt{\boldsymbol{k}^2+M_{\rm U_V}^2}\right)t}}{\sqrt{(\boldsymbol{p}+\boldsymbol{k})^2+M_{\rm U_V}^2}\sqrt{\boldsymbol{k}^2+M_{\rm U_V}^2}}\right.\\
&\quad+C_{\rm V_\eta}^2\frac{{\rm e}^{-\left(\sqrt{(\boldsymbol{p}+\boldsymbol{k})^2+M_{\rm \eta V}^2}+\sqrt{\boldsymbol{k}^2+M_{\rm \eta V}^2}\right)t}}{\sqrt{(\boldsymbol{p}+\boldsymbol{k})^2+M_{\rm \eta V}^2}\sqrt{\boldsymbol{k}^2+M_{\rm \eta V}^2}}\\
&\quad+C_{\rm V_{\eta'}}^2\frac{{\rm e}^{-\left(\sqrt{(\boldsymbol{p}+\boldsymbol{k})^2+M_{\rm \eta' V}^2}+\sqrt{\boldsymbol{k}^2+M_{\rm \eta' V}^2}\right)t}}{\sqrt{(\boldsymbol{p}+\boldsymbol{k})^2+M_{\rm \eta' V}^2}\sqrt{\boldsymbol{k}^2+M_{\rm \eta' V}^2}}\\
&\quad-C_{\rm V_\eta}C_{\rm V_{\eta'}}\frac{{\rm e}^{-\left(\sqrt{(\boldsymbol{p}+\boldsymbol{k})^2+M_{\rm \eta V}^2}+\sqrt{\boldsymbol{k}^2+M_{\rm \eta' V}^2}\right)t}}{\sqrt{(\boldsymbol{p}+\boldsymbol{k})^2+M_{\rm \eta V}^2}\sqrt{\boldsymbol{k}^2+M_{\rm \eta' V}^2}}\\
&\quad\left.-C_{\rm V_\eta}C_{\rm V_{\eta'}}\frac{{\rm e}^{-\left(\sqrt{(\boldsymbol{p}+\boldsymbol{k})^2+M_{\rm \eta' V}^2}+\sqrt{\boldsymbol{k}^2+M_{\rm \eta V}^2}\right)t}}{\sqrt{(\boldsymbol{p}+\boldsymbol{k})^2+M_{\rm \eta' V}^2}\sqrt{\boldsymbol{k}^2+M_{\rm \eta V}^2}}\right\},
\end{aligned}$$

$$f_{\rm B}(\boldsymbol{p},t)\equiv\sum_{\boldsymbol{k}}\Bigg\{\frac{1}{9}\frac{{\rm e}^{-\left(\sqrt{(\boldsymbol{p}+\boldsymbol{k})^2+M^2_{\eta{\rm I}}}+\sqrt{\boldsymbol{k}^2+M^2_{\eta{\rm I}}}\right)t}}{\sqrt{(\boldsymbol{p}+\boldsymbol{k})^2+M^2_{\eta{\rm I}}}\sqrt{\boldsymbol{k}^2+M^2_{\eta{\rm I}}}}$$
$$-\frac{{\rm e}^{-\left(\sqrt{(\boldsymbol{p}+\boldsymbol{k})^2+M^2_{\rm U_I}}+\sqrt{\boldsymbol{k}^2+M^2_{\rm U_I}}\right)t}}{\sqrt{(\boldsymbol{p}+\boldsymbol{k})^2+M^2_{\rm U_I}}\sqrt{\boldsymbol{k}^2+M^2_{\rm U_I}}}$$
$$+\frac{1}{16}\sum_{b=1}^{16}4\frac{{\rm e}^{-\left(\sqrt{(\boldsymbol{p}+\boldsymbol{k})^2+M^2_{\rm U_b}}+\sqrt{\boldsymbol{k}^2+M^2_{\rm U_b}}\right)t}}{\sqrt{(\boldsymbol{p}+\boldsymbol{k})^2+M^2_{\rm U_b}}\sqrt{\boldsymbol{k}^2+M^2_{\rm U_b}}}$$
$$+\frac{1}{16}\sum_{b=1}^{16}\frac{{\rm e}^{-\left(\sqrt{(\boldsymbol{p}+\boldsymbol{k})^2+M^2_{\rm K_b}}+\sqrt{\boldsymbol{k}^2+M^2_{\rm K_b}}\right)t}}{\sqrt{(\boldsymbol{p}+\boldsymbol{k})^2+M^2_{\rm K_b}}\sqrt{\boldsymbol{k}^2+M^2_{\rm K_b}}}\Bigg\},$$

where $\delta_{\rm V}$, $\delta_{\rm A}$, B_0, $C_{{\rm V}_\eta}$, $C_{{\rm V}_{\eta'}}$, $C_{{\rm A}_\eta}$, $C_{{\rm A}_{\eta'}}$ are constants, which are given in the above subsection, and for $f_{\rm A}^{\rm hairpin}(t)$, we just require ${\rm V}\to{\rm A}$ in $f_{\rm V}^{\rm hairpin}(t)$.

4 Simulations and results

In the present work we analyzed the MILC fine ($a=0.09$ fm) lattice ensemble of 500 $28^3\times 96$ gauge configurations generated in the presence of $2+1$ flavors of Asqtad improved staggered quarks with bare quark masses $am_{\rm ud}=0.0062$ and $am_{\rm s}=0.031$ and bare gauge coupling $10/g^2=7.09$ [17].

We set valence quark masses equal to the sea quark masses. Table 1 gives the pseudoscalar masses used in our fits with the exception of the masses $M_{\eta_{\rm A}}$, $M_{\eta'_{\rm A}}$, $M_{\eta_{\rm V}}$, $M_{\eta'_{\rm V}}$. Those masses vary with the fit parameters $\delta_{\rm A}$ and $\delta_{\rm V}$.

After we perform the Wick contractions of the fermion fields, and sum over the index of the taste replica for Eqs. (6) and (11), for the light quark Dirac operator $M_{\rm u}$, we measure the point-to-point quark-line connected correlator

$$C_{\rm CC}(\boldsymbol{p},t)=\sum_{\boldsymbol{x}}(-)^x{\rm e}^{{\rm i}\boldsymbol{p}\cdot\boldsymbol{x}}\times\left\langle{\rm Tr}\left[M_{\rm u}^{-1}(\boldsymbol{x},t;0,0)M_{\rm u}^{-1^\dagger}(\boldsymbol{x},t;0,0)\right]\right\rangle,\tag{13}$$

and the point-to-point quark-line disconnected correlator

$$C_{\rm DC}(\boldsymbol{p},t)=\sum_{\boldsymbol{x}}(-)^x{\rm e}^{{\rm i}\boldsymbol{p}\cdot\boldsymbol{x}}\times\langle{\rm Tr}M_{\rm u}^{-1}(\boldsymbol{x},t;\boldsymbol{x},t){\rm Tr}M_{\rm u}^{-1}(0,0;0,0)\rangle.\tag{14}$$

In the latter case we use noisy estimators based on random color fields [25] ξ_i for $i=1,\cdots,N=100$:

$$\begin{aligned}&{\rm Tr}M_{\rm u}^{-1}(\boldsymbol{x},t;\boldsymbol{x},t){\rm Tr}M_{\rm u}^{-1}(0,0;0,0)\\ \approx&\frac{1}{N(N-1)}\sum_{i\neq i',y,y'}\bar{\xi}_{\rm k}(\boldsymbol{x},t)M_{\rm u}^{-1}(\boldsymbol{x},t;y)\xi_i(y)\\ &\times\bar{\xi}_{i'}(0,0)M_{\rm u}^{-1}(0,0;y')\xi_{i'}(y').\end{aligned}\tag{15}$$

We use the conjugate gradient method (CG) to obtain the required matrix element of the inverse fermion matrix $M_{\rm u}$. In order to improve the statistics, when we calculate the connected part, we compute the correlators from eight source time slices evenly spread through the lattice (i.e., only one source time slice is chosen at a time), and average the correlators. In terms of these correlators the timeslice a_0 and f_0 correlators are

$$\begin{aligned}C_{\rm a_0}(\boldsymbol{p},t)=&\ C_{\rm CC}(\boldsymbol{p},t),\\ C_{\rm f_0}(\boldsymbol{p},t)=&\ C_{\rm CC}(\boldsymbol{p},t)-\frac{1}{2}C_{\rm DC}(\boldsymbol{p},t).\end{aligned}\tag{16}$$

Correlators in each channel are measured at five momenta $\boldsymbol{p}=(0,0,0)$, $(1,0,0)$, $(1,1,0)$, $(1,1,1)$, and $(2,0,0)$. In this work we also measure the $\langle\psi\bar{\psi}\rangle$. All ten correlators are then fit to the following model

$$\begin{aligned}C_{\rm a_0}(\boldsymbol{p},t)=&\ C^{\rm meson}_{\rm a_0}(\boldsymbol{p},t)+B_{\rm a_0}(\boldsymbol{p},t),\\ C_{\rm f_0}(\boldsymbol{p},t)=&\ C^{\rm meson}_{\rm f_0}(\boldsymbol{p},t)+B_{\rm f_0}(\boldsymbol{p},t),\end{aligned}\tag{17}$$

where

$$\begin{aligned}C^{\rm meson}_{\rm a_0}(\boldsymbol{p},t)=&\ b_{\rm a_0}(\boldsymbol{p})e^{-E_{\rm a_0}(\boldsymbol{p})t}\\ &+b_{\pi{\rm A}}(\boldsymbol{p})(-)^t{\rm e}^{-E_{\pi_{\rm A}}(\boldsymbol{p})t}+(t\to N_{\rm t}-t),\\ C^{\rm meson}_{\rm f_0}(\boldsymbol{p},t)=&\ c_0(\boldsymbol{p})+b_{\rm f_0}(\boldsymbol{p}){\rm e}^{-E_{\rm f_0}(\boldsymbol{p})t}\\ &+b_{\eta_{\rm A}}(\boldsymbol{p})(-)^t{\rm e}^{-E_{\eta_{\rm A}}(\boldsymbol{p})t}+(t\to N_{\rm t}-t).\end{aligned}$$

This fitting model includes the explicit a_0 and f_0 poles, as well as the corresponding negative parity states, and the bubble contribution. The constant $c_0(p)$ is the vacuum expectation value for the f_0 correlator, hence it is zero for all momenta except $\boldsymbol{p}=(0,0,0)$, in which case it gives the vacuum-disconnected part of the f_0 correlator.

As discussed in Ref. [21], we chose the empirical fitting form for the parameterization of the momentum dependence of the overlap factors. In this work we concentrate on the other physical fitting parameters, hence we just fit the data of the momentum

$\boldsymbol{p}=(0,0,0)$, thus

$$C^{\rm meson}_{\rm a_0}(t) = b_{\rm a_0}{\rm e}^{-E_{\rm a_0}t}+b_{\pi{\rm A}}(-)^t{\rm e}^{-E_{\pi_{\rm A}}t}+(t\to N_{\rm t}-t),$$

$$C^{\rm meson}_{\rm f_0}(t) = c_0+b_{\rm f_0}{\rm e}^{-E_{\rm f_0}t}+b_{\eta_{\rm A}}(-)^t{\rm e}^{-E_{\eta_{\rm A}}t} +(t\to N_{\rm t}-t).$$

There are nine fit parameters for the meson terms alone, but the two negative-parity masses were constrained tightly by priors: the $\pi_{\rm A}$, to the previously measured value, and the $\eta_{\rm A}$, to the same derived mass that we used in the bubble term.

The bubble terms $B_{\rm a_0}(\boldsymbol{p},t)$ and $B_{\rm f_0}(\boldsymbol{p},t)$ were parameterized by the three low-energy couplings $B_0 = m_\pi^2/(2m_{\rm u})$, $\delta_{\rm A}$, and $\delta_{\rm V}$ in the notation of Ref. [15]. They were allowed to vary to give the best fit. The taste multiplet masses in the bubble terms were fixed as noted above. The sum over intermediate momenta was cut off when the total energy of the two-body state exceeded $1.8/a$ or any momentum component exceeded $\pi/(3a)$. We determined that such a cutoff gave an acceptable accuracy for $t\geqslant 6$.

In summary, we simultaneously fitted all two correlators with eleven parameters, nine of which were needed to parameterize the four explicit meson terms, and three low-energy couplings were needed for the bubble contribution. Our best fit gave χ^2/dof= 26.4/22.

The fitted functional form is compared with the data in Figs. 1–2.

The results of the three fitted low-energy couplings are compared with the results from fits to the meson masses and decay constants in Table 2. In Ref. [21], through a prior, we constrained the value of $\delta_{\rm V}$ to conform to previous fits to the pseudoscalar masses and decay constants [15], leaving only two of the low energy couplings to be adjusted independently. The agreement is worse if we let the value of $\delta_{\rm V}$ vary. In this work we let all the three low-energy couplings be adjusted independently, and achieve chiral couplings that are well consistent with previous determinations. This suggests, perhaps, that for the coarse ($a=0.12$ fm) lattice ensemble a higher-order calculation of the bubble contribution might improve the agreement, and for the fine ($a=0.09$ fm) lattice ensemble the bubble contribution with low order is enough.

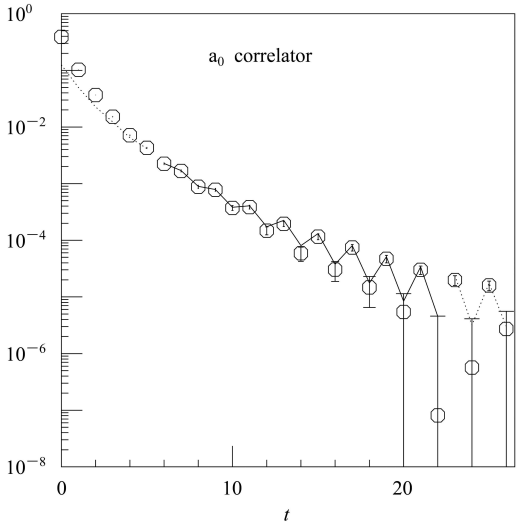

Fig. 1. The best fit to the $\rm a_0$ correlator for zero cm momentum. The fitting range is indicated by points and fitted solid lines. We shift all the points and fitted lines $6{\rm e}-6$ in y axis for good visualization.

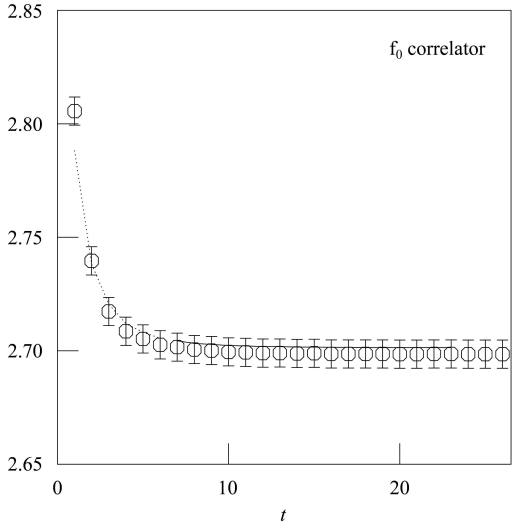

Fig. 2. The best fit to the zero momentum $\rm f_0$ correlator. The fitting range is indicated by points and fitted solid lines.

Table 2. Comparison of our fit parameters for the rSχPT couplings with the results from [15].

	our fit	meson masses and decays
$r_1 m_\pi^2/(2m_{\rm u,d})$	7.2(1.4)	6.5
$\delta_{\rm V}$	−0.0053(10)	−0.0056(80)
$\delta_{\rm A}$	−0.0137(19)	−0.014(2)

In Ref. [15] the values of $\delta_{\rm A}$ and $\delta_{\rm V}$ on the fine lattices are not fitted separately but are constrained to be 0.35 times as large for the central-value fits. Our fitted results confirm this estimations.

As is computed in Eq. (37) in Ref. [21], the quark-line disconnected correlator includes the vacuum disconnected piece which does not vanish,that is,

$$c_0 = \frac{L^3}{2}\left\langle\psi\bar{\psi}\right\rangle^2, \qquad (18)$$

where we consider the factor 1/2 for the disconnected part in Eq. (16), and the normalization $M = 2D+2am$ for the Dirac matrix. In this work, we have also measured the value of $\langle\psi\bar{\psi}\rangle$, which is in good agreement with the value in Ref. [26], i.e., $\langle\psi\bar{\psi}\rangle = 0.015622(17)$. Hence we can estimate its value as $c_0 = 2.697(5)$. The fitted c_0 is 2.701(6).

The fitted masses of the a_0 and f_0 in units of the lattice spacing are 0.59(3) and 0.35(4), respectively.

5 Summary and outlook

In Refs. [20, 21], we derived the two-pseudoscalar-meson "bubble" contribution to the a_0 and f_0 correlators in the lowest order SχPT. We have used this model to fit the simulation data for the point-to-point a_0 and f_0 correlators for the fine ($a = 0.09$ fm) lattice ensemble and found that the best-fit values of all the three chiral low-energy couplings are in good agreement with the values previously obtained in fits to the light meson spectra and decay constants [15].

The two-meson bubble term in SχPT provides a useful explanation of the lattice artifacts induced by the fourth-root approximation [20, 21]. The artifacts include thresholds at unphysical energies and thresholds with negative weights. These contributions are still clearly present in the a_0 and f_0 channels in our QCD simulation with the Asqtad action at $a = 0.09$ fm. We have found that the "bubble" term must be included in a successful spectral analysis.

The rSχPT further predicts that these lattice artifacts disappear in the continuum limit, leaving only the physical two-body thresholds. This result is in full accord with the fourth-root analysis of Ref [2]. Although we have minimized the lattice artifacts by using an improved action with the fine ($a = 0.09$ fm) lattice ensemble, an empirical investigation of these effects is necessary. It would be very nice to be able to see whether this expectation is ruled out in numerical QCD simulations at much smaller lattice spacing. We are beginning a series of simulations with a MILC super-fine $a = 0.06$ fm lattice ensemble to investigate these effects.

We wish to thank the MILC Collaboration for the use of the Asqtad lattice ensemble. We are grateful to Hou Qing for his support. Computation for this work was performed at the AMAX workstation and HP workstation in the Radiation Physics Group of the Institute of Nuclear Science and Technology, Sichuan University.

References

1 Bernard C, Golterman M, Shamir Y. Phys. Rev. D, 2006, **73**: 114511
2 Bernard C. Phys. Rev. D, 2006, **73**: 114503
3 Shamir Y. Phys. Rev. D, 2007, **75**: 054503
4 Stephen R. Sharpe. PoS, LAT2006, 2006. 022
5 Bernard C, Golterman M, Shamir Y. PoS, LAT2006. 2007. 205
6 Durr S, Hoelbling C. Phys. Rev. D, 2004, **69**: 034503
7 Follana E, Hart A, Davies C T H. Phys. Rev. Lett., 2004, **93**: 241601
8 Follana E, Hart A, Davies C T H, Mason Q. Phys. Rev. D, 2005, **72**: 054501
9 Durr S, Hoelbling C, Wenger U. Phys. Rev. D, 2004, **70**: 094502
10 Durr S, Hoelbling C. Phys. Rev. D, 2005, **71**: 054501
11 Bernard C et al. PoS, LAT2005. 2006. 114
12 Bernard C et al. PoS, LAT2006, 2007. 163
13 Aubin C, Bernard C. Phys. Rev. D, 2003, **68**: 034014
14 Aubin C, Bernard C. Phys. Rev. D, 2003, **68**: 074011
15 Aubin C et al. Phys. Rev. D, 2004, **70**: 114501
16 Billeter B, DeTar C, Osborn J. Phys. Rev. D, 2004, **70**: 077502
17 Aubin C et al. Phys. Rev. D, 2004, **70**: 094505
18 Prelovsek S. PoS, LAT2005, 2006. 085
19 Prelovsek S. Phys. Rev. D, 2006, **73**: 014506
20 FU Zi-Wen. Hybrid Meson Decay from the Lattice. UMI-32-34073, 2006
21 Bernard C. Phys. Rev. D, 2007, **76**: 094504
22 Aubin C, Bernard C. Nucl. Phys. Proc. Suppl., 2004, **129**: 182
23 Bernard C W et al. Phys. Rev. D, 2001, **64**: 054506
24 Damgaard P H, Splittorff K. Phys. Rev. D, 2000, **62**: 054509
25 DONG Shao-Jing, LIU Ke-Fei. Phys. Lett. B, 1994, **328**: 130
26 Bazavov A et al. Rev. Mod. Phys., 2010, **82**: 1349